International Journal of Automation and Computing 16(3), June 2019, 261-273
DOI: 10.1007/s11633-018-1161-8

Development and Modeling of Remotely Operated Scaled Multi-wheeled Combat Vehicle Using System Identification

A. N. Ouda Amr Mohamed Moustafa EI-Gindy Haoxiang Lang Jing Ren

Faculty of Engineering and Applied Science, University of Ontario Institute of Technology (UOIT), Oshawa L1H7K4, Canada

Abstract: This paper describes the development and modeling of a remotely operated scaled multi-wheeled combat vehicle (ROMWCV) using system identification methodology for heading angle tracking. The vehicle was developed at the vehicle dynamics and crash research (VDCR) Lab at the University of Ontario Institute of Technology (UOIT) to analyze the characteristics of the full-size model. For such vehicles, the development of controllers is considered the most crucial issue. In this paper, the ROMWCV is developed first. An experimental test was carried out to record and analyze the vehicle input/output signals in open loop system, which is considered a multi-input-single-output (MISO) system. Subsequently, a fuzzy logic controller (FLC) was developed for heading angle tracking. The experiments showed that it was feasible to represent the dynamic characteristics of the vehicle using the system identification technique. The estimation and validation results demonstrated that the obtained identified model was able to explain 88.44% of the output variation. In addition, the developed FLC showed a good heading angle tracking.

Keywords: Autonomous multi-wheeled vehicle, system identification, all wheel steering, fuzzy logic (FL), parametric identification.

1 Introduction

The past decade has witnessed an unprecedented development in the field of unmanned ground vehicles (UGVs) including wide applications for both civilian and military fields. Generally, an UGV is a self-driving vehicle that has the capability to observe and understand the surrounding environment. UGVs are used to replace humans in hazardous situations. Consequently, unmanned combat vehicles have been receiving great attention in recent research due to their important applications in the military. Building such vehicles has drawn dramatic attention which is one of the motivating topics in both robotics and automotive engineering research[1, 2].

The expected outcomes from applying autonomy to such vehicles are set to increase the combat capability and maintain soldier safety in different battlefield scenarios. Obtaining an accurate mathematical model of the vehicle to be controlled is considered the main challenge. For this purpose, system identification techniques are introduced in order to solve such problems.

System identification methodology was introduced to study the performance of a developed dynamic system and estimate its mathematical model by observing input/output signals[3]. These signals consist of a mathematical expression that precisely defines the input and output relationship. System identification has a long history in solving significant problems in the field of autonomous systems and robotics. For example, system identification has been used in the following kinematic problems: modeling and calibration of robotic manipulators[4–9], parameter identification and nonlinear modeling[10–13], adaptive control and neural network-based system identification[14–18], estimation of inertial parameters[19–21], and the prediction of the environment[22].

Eng et al.[23] introduced online identification for an autonomous underwater vehicle dynamics model using an experimental test. This vehicle was commanded to execute a compact set of maneuvers under doublet excitation. In addition, Garg et al.[24] discussed several modeling methods and types of models using system identification such as black-box, gray-box, white-box, and parametric, non-parametric system identification. Lai and Tri[25] developed a system identification model to identify the pitch, roll and yaw dynamic models for a small unmanned helicopter, then a software-in-the-loop was developed for the estimated model.

Mendes and Medeiros[26] introduced an identification model of a wheeled mobile robot with a differential drive. The robot has been modeled by multiple input and single output (MISO) Hammerstein systems with input dead zones. The robot dynamic model is based on the traveled distance increment instead of the robot coordinates, making the model linear and allowing the application of classical methods of identification. Both parameters of linear and nonlinear blocks are estimated simultaneously through application of recursive least squares. Hasiewics et al.[27] developed a system identification model for block-oriented dynamic nonlinear systems. The Hammerstein and

Research Article
Manuscript received May 8, 2018; accepted October 8, 2018; published online February 28, 2019
Recommended by Associate Editor Ding-Li Yu

Wiener system has been investigated. In addition, the advantages of parametric and non-parametric identification techniques were discussed.

The development of controllers for autonomous vehicles has been widely studied by researchers around the world. Fuzzy logic (FL) is a powerful controller for use with complex systems based on expert human knowledge. FL algorithms are used to control autonomous systems in many engineering fields[28–31]. Furthermore, the main advantages of using FL include easy implementation, efficient computation and better performance[32].

Wang et al.[33] developed a fuzzy logic controller for autonomous bay parking. The authors investigated the available parking space dimensions and the kinetic model was set up for the case when the backward or forward speed was low. Two fuzzy algorithms were developed. The first controller was used to control the speed and the other one was for steering control. Antonelli et al.[34] introduced a path-following algorithm based on a fuzzy logic controller. The proposed controller emulates human driving behavior. The controller uses the information of the curvature of the desired path ahead and the distance between the vehicle and the next bend in order to drive the vehicle safely. On the other hand, the controller output is the maximum value of the linear velocity.

Sahoo et al.[35] designed a controller for tracking the desired heading angle for an unmanned ground vehicle considering the limits on rotation of steering wheel and steering motor rate. A two-degree-of-freedom vehicle model is considered for the controller design.

In this paper, the main contribution is the development and modelling of a remotely operated scaled multi-wheeled combat vehicle using system identification techniques in order to control the vehicle heading angle. The main challenge of designing such control systems is to individually regulate the steering of the four front wheels in the same order for obtaining the predefined heading angle of the vehicle. The developed vehicle is an electric-powered 1: 6 scale model of an 8×8 full combat vehicle. It has eight wheels that are all independently driven by electric motors and can perform multiple steering methods, which can be controlled remotely using a radio controller. First, the remotely operated scaled multi-wheeled combat vehicle (ROMWCV) is developed and the input/output signals are recorded and analyzed on an open loop system through the experimental test. The vehicle dynamic model was identified by applying system identification methods considering autoregressive exogeneous (ARX), autoregressive moving average exogeneous (ARMAX), box-jenkins (BJ), output error (OE), state-space (SS), and transfer function (TF) models. Subsequently, a fuzzy logic controller (FLC) is applied to control the identified vehicle model and follow the desired heading angle. Several statistical analyses are applied, and the results are compared in order to identify and control the suitable vehicle model.

2 Remotely operated scaled multi-wheeled combat vehicle

The complete remotely operated scaled multi-wheeled combat vehicle system is shown in Fig. 1 (a), while the actual one is shown in Fig. 1 (b). This vehicle is developed at the vehicle dynamics and crash research (VDCR) Laboratory at the University of Ontario Institute of Technology (UOIT)[36]. The developed vehicle is a 1: 6 scale model of an 8×8 electric combat vehicle that can perform multiple steering modes to meet situational needs. In addition, all eight wheels are powered individually.

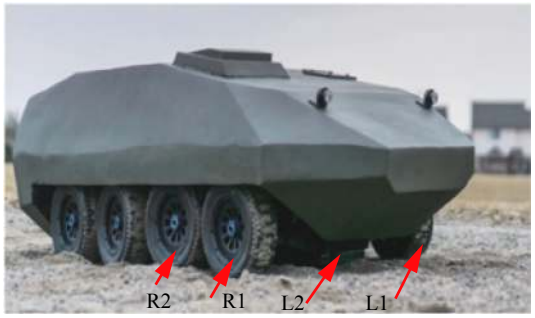

(a) Remotely operated scaled multi-wheeled combat vehicle

(b) Actual vehicle

Fig. 1 Multi-wheeled combat vehicle

The vehicle has three levels, the first level contains the eight direct current (DC) motors and electronic speed controllers (ESCs) as shown in Fig. 2 (a). The middle level is the steering layer as shown in Fig. 2 (b). This level contains eight steering servos that are also connected by a DB25 connector. At the top as shown in Fig. 2 (c), there are 4 batteries that are connected to the scalable power bus that all ESCs are connected. In addition, a microcontroller is used to connect the gateway board to the two harnesses from the servos and ESCs. The inertial measurement unit (IMU) is placed under the gateway board enclosure as it should be as centered as possible.

2.1 Powertrain hardware architecture

In this section, the hardware architecture for the elec-

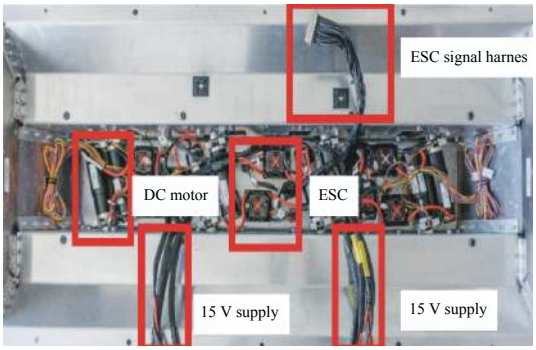

(a) Chassis first level

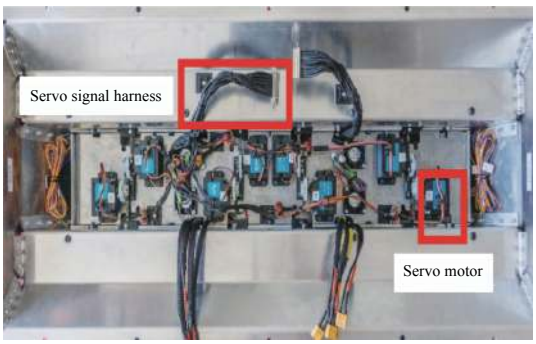

(b) Chassis middle level

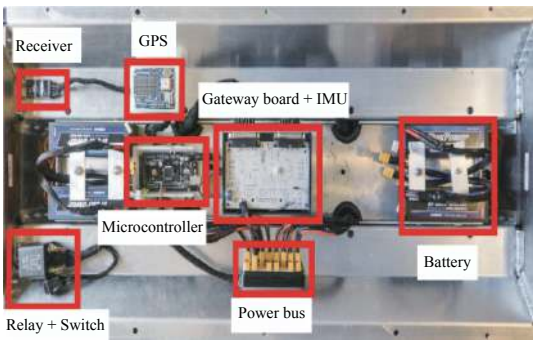

(c) Chassis top level

Fig. 2 Vehicle component

tronic powertrains is discussed. There are two microcontrollers introduced in this design. The primary one is used to control the vehicle by receiving the driver request via the radio receiver. In addition, it is calculating the corresponding outputs for the steering servo motors as well as the driving DC motors as shown in Fig. 3. The connection between the microcontroller and the motors is established using a pulse width modulation (PWM) channel. Each DC motor is individually controlled by an electronic speed controller that draws its power from the power system.

The second microcontroller is used to connect the global positioning system (GPS) and IMU with the primary controller and handles the data logging and processing. The circuit diagram of the powertrain as seen from above with each pin connection labeled is shown in Fig. 4.

The complete ROWMCV system is represented in Fig. 5. Fig. 5 provides an overview of the vehicle control system, starting by sending the command signal from the remote control to the radio receiver by the corresponding vehicle action. The microprocessor receives the command signal, then calculates the corresponding output for the four front wheels in order to control and navigate the vehicle in the desired direction.

2.2 Vehicle features

The features of the remotely operated scaled multi-wheeled combat vehicle capabilities are as follows[36]:

1) This vehicle is capable of forward and backward movement where all eight wheels are powered individually.

2) Alternate between three unique steering configurations.

3) Have the capability to operate under extreme conditions such as summer heat waves, winter freezes.

4) Provide sufficient ground clearance to overcome obstacles like large objects.

5) Capability to steer on multiple surfaces such as sand, dirt, snow, mud and pavement.

6) High maneuverability to operate in confined areas.

7) Able to climb over steep terrain and reach moderate speeds similar to that of the full model.

3 System identification (SI)

Generally, SI is the process of modelling system dynamics based on the measured input/output signals via an experimental test. It has the capability to provide an accurate mathematical model of the system dynamics. The SI approach has five steps[29] as shown in Fig. 6: 1) experimental design, 2) data retrieval, 3) parameter estimation algorithm and system identification model selection, 4) model validation, 5) model implementation. If the model validation is not good enough to represent the actual model of the system dynamics, the first three steps will be repeated again until the model validation achieves the assigned level of accuracy.

System identification using parametric identification techniques has a specific model structure. The parameters are estimated using the observation of the input/output data. In addition, it is providing a large variety and possibilities regarding different ways of describing the system, where the output of system $Y(Z)$ can be defined as follows.

$$Y(z) = G(z)X(z) + M(z). \tag{1}$$

Equation (1) can be rewritten as follows:

$$Y(z) = G(z)X(z) + H(z)E(z) = \frac{N(z)}{D(z)}X(z) + \frac{A(z)}{B(z)}E(z) \tag{2}$$

where

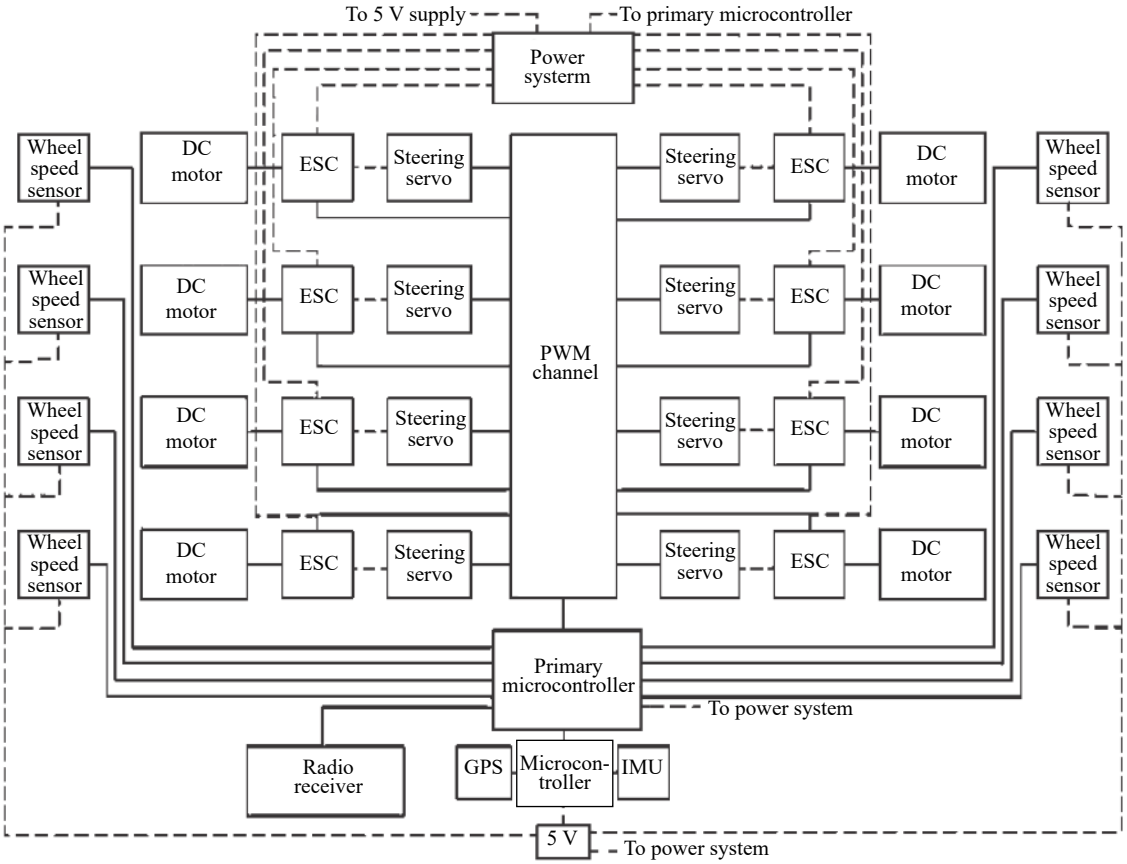

Fig. 3 Hardware architecture

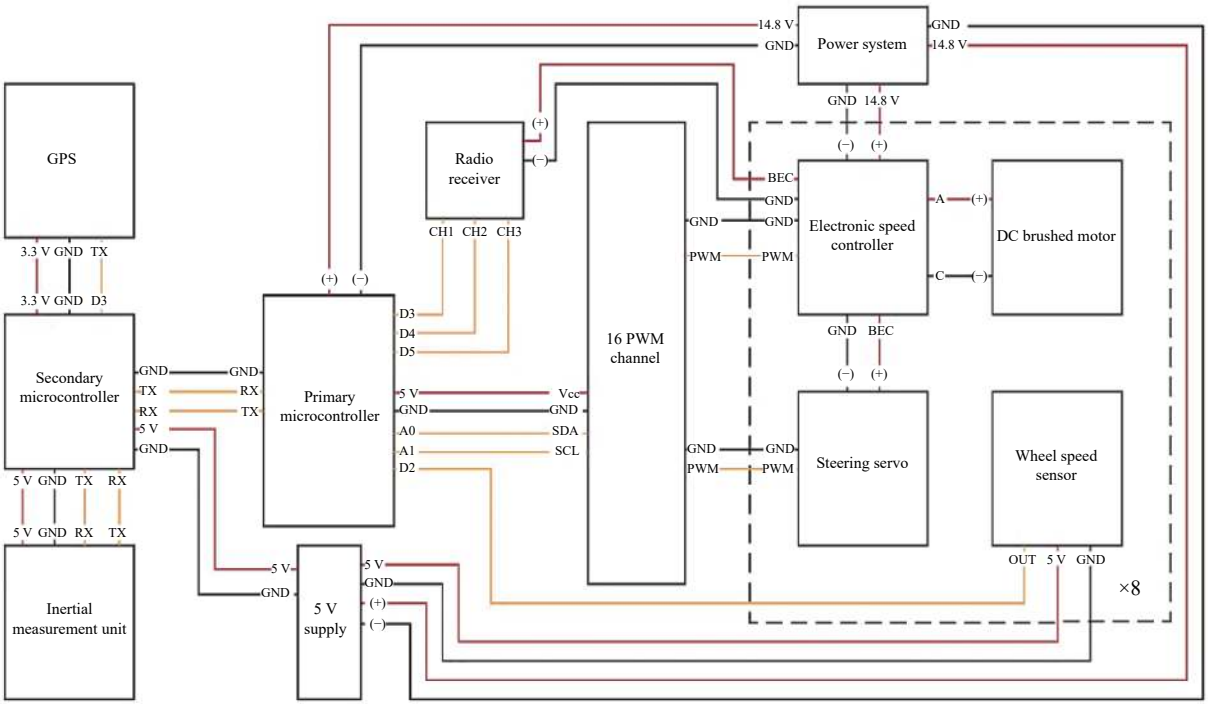

Fig. 4 Powertrain circuit diagram (Color versions of the figures in this paper are available online)

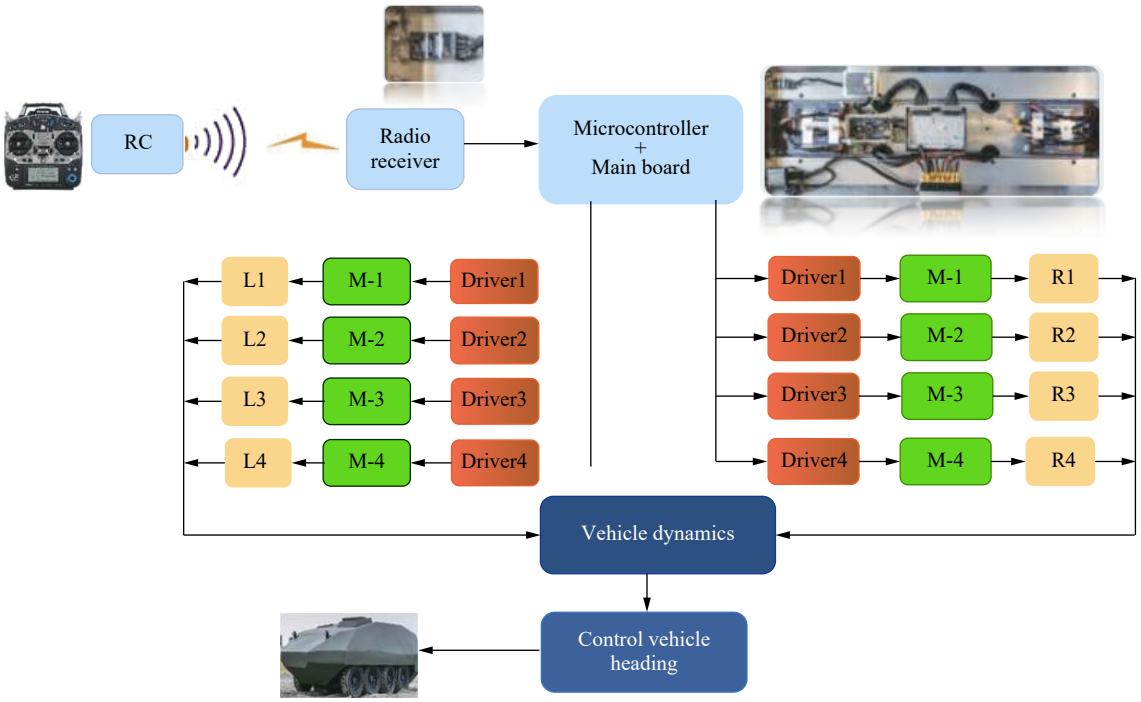

Fig. 5 ROMWCV's system

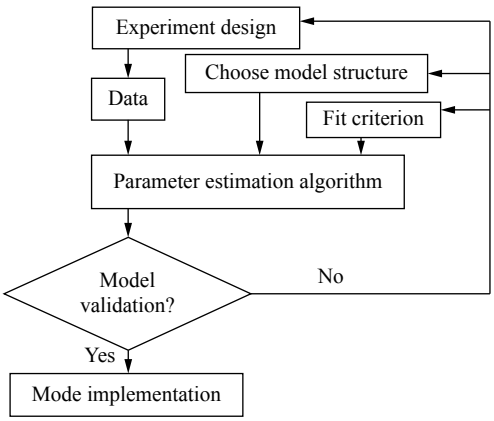

Fig. 6 System identification procedure

$Y(z)$ is the n_y output,
$X(z)$ is the n_x input,
$E(z)$ is the transform of a white noise,
$G(z)$ is the transfer function of the system,
$H(z)$ is the stochastic behavior of noise.

The modeling of ROMWCV will be considered by applying ARX, ARMAX, BJ, OE, SS and TF models. The characteristics of each model were studied in [37].

The ARX model in (3) is considered the simplest estimation model as shown in Fig. 7. The main weakness is the disturbance model $\frac{1}{N(z)}$ that comes with the system's poles. Consequently, an incorrect estimation of the system dynamics can be accrued due to the term A in (2). Accordingly, this issue can be avoided by the requirement of higher orders coefficients of terms A and B, where the signal to noise ratio is acceptable.

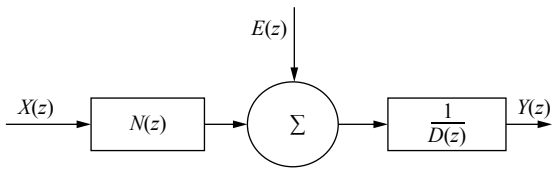

Fig. 7 ARX model

$$D(z)Y(z) = N(z)X(z) + E(z). \tag{3}$$

The ARMAX model in (4) has the capability of handling the disturbance modeling compared with ARX model. For this purpose, ARMAX is considered the most popular model that can be used in many applications. The block diagram of the ARMAX model is shown in Fig. 8.

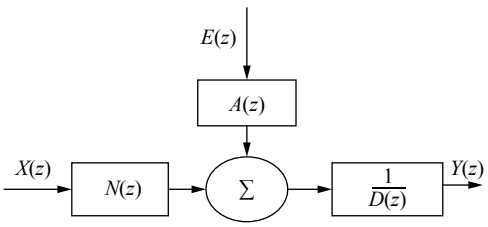

Fig. 8 ARMAX model

$$D(z)Y(z) = N(z)X(z) + A(z)E(z). \tag{4}$$

The OE models (5) and the block diagram of the OE model is shown in Fig. 9. This model is able to describe the dynamics of the system separately. Meanwhile, there are no wasted parameters on the disturbance model. The main advantage of this model is that it is able to estim-

ate the correct transfer function $G(z)=\dfrac{N(z)}{D(z)}$, if there isn't feedback during collecting the data.

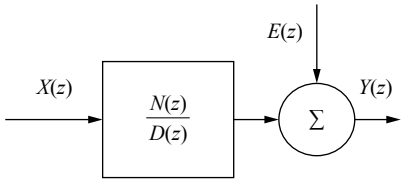

Fig. 9 OE model

$$Y(z)=\left[\frac{N(z)}{D(z)}\right]X(z)+E(z). \tag{5}$$

The disturbance properties of the BJ model are modeled separately from the system dynamics. The block diagram of the BJ model is shown in Fig. 10.

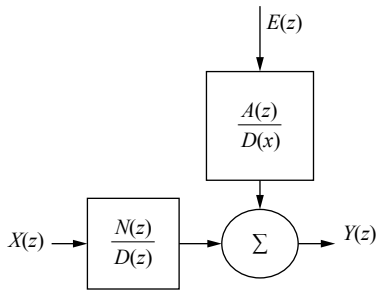

Fig. 10 BJ model

$$Y(z)=\left[\frac{N(z)}{D(z)}\right]X(z)+\left[\frac{A(z)}{B(z)}\right]E(z). \tag{6}$$

Using the SS model, the state-space form is the best way to describe a linear system as described in (7).

$$\begin{aligned}\dot{x}&=Ax(t)+Bu(t)\\ y(t)&=Cx(t)+Du(t)+v(t)\end{aligned} \tag{7}$$

where the relationship between the input $u(t)$ and the output $y(t)$ is defined via the nx-dimensional state vector $x(t)$.

3.1 System identification algorithm

System identification starts by selecting a model structure followed by the computation of an appropriate model in the structure. The selected model will be evaluated afterward. Fig. 11 shows this process which can be summarized as follows:

Step 1. Record the input/output signals to/from the vehicle.

Step 2. Examine the data and select useful portions of the original data.

Step 3. Estimate input delay to gain a better insight into the dynamics via obtaining the impulse response of the system.

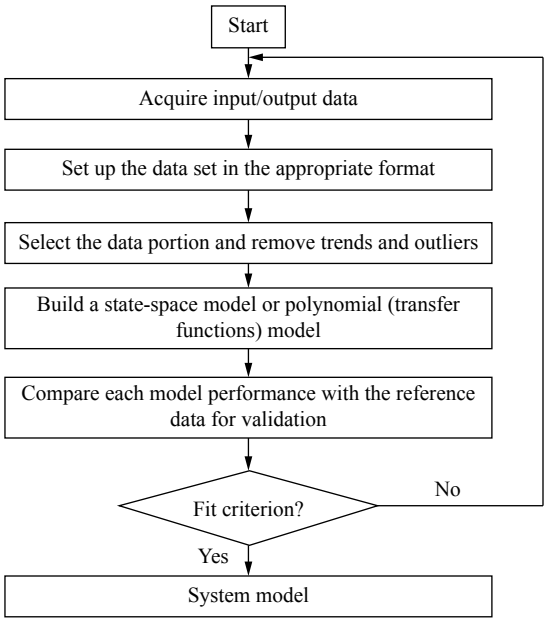

Fig. 11 System identification procedure flowchart

Step 4. Select and define the appropriate identification model structure within which the model of the system can be obtained.

Step 5. Choose the best model structure corresponding to the input/output data and the given fit to estimation criterion.

Step 6. Examine the obtained model's properties (pole-zero configurations).

Step 7. If the selected model is good enough to represent the identified system, then stop, otherwise go back to the fourth step, to try another model set. Possibly also try another estimation method in the fifth step or work further on the input-output data obtained in first and second steps.

3.2 Experimental setup

In this section, the experimental setup for recording and analyzing the input/output signals will be discussed. A tilt compensated magnetic compass (CMPS11) is used to provide the vehicle Euler angles as shown in Fig. 12. It has three magnetometers, three gyros, and three accelerometers. The main advantage of this sensor is that it uses a Kalman filter (KF). This KF is used to integrate the gyro and accelerometer to avoid the errors that may be accrued by printed circuit board (PCB) tilting. The CMPS11 will be interfaced with an Arduino to save the obtained input/output signals data on an secure digital card (SD card) during the test as shown in Figs. 13 (a) and 13 (b).

The road test of the ROMWCV was carried out on pavement surface as shown in Fig. 14, where the vehicle heading angle is controlled in open loop test via the remote control. In order to obtain reliable data, the vehicle

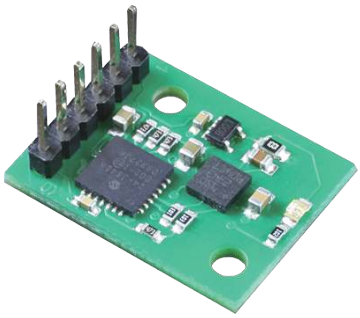

Fig. 12 Tilt compensated magnetic compass (CMPS11)

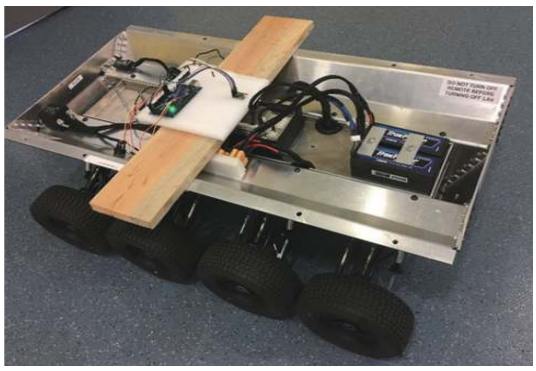

(a) COMP11 connected to arduino

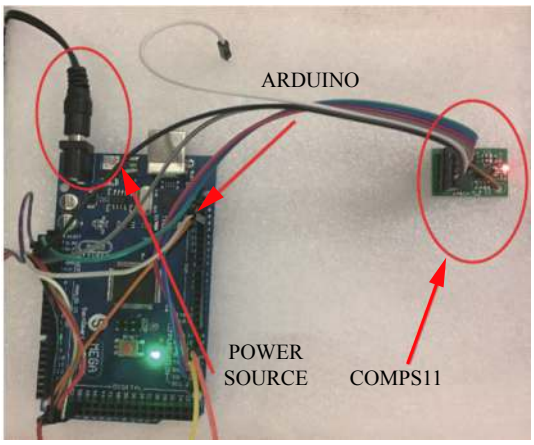

(b) Sensors fitted to ROMWCV

Fig. 13 Experiment test

heading angle should be changed continuously during the maneuver. This test was repeated for five times to make sure that the recorded input/output signals is accurate when applying the system identification technique.

4 Simulation and results

In this section, the ROMWCV input/output data is recorded and analyzed to deduce a model as shown in Fig. 15. The right and left wheels of the first axle are represented by R1 and L1, while R2 and L2 represent the second axle.

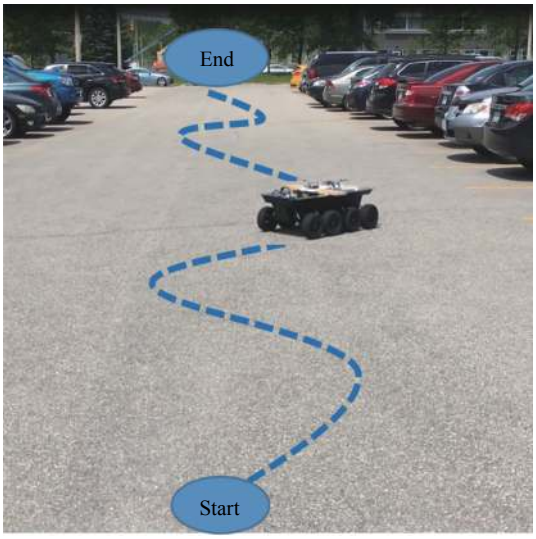

Fig. 14 Road test

The system identification toolbox using Matlab software will be used to develop the vehicle model. First, the data is loaded on to a Matlab command window, the recorded inputs and output data are set, then the command "ident" opens the system identification toolbox interface.

The step response of the ROMWCV will be displayed as shown in Fig. 16 which represent the vehicle input/output relations.

The ARX, ARMAX, BJ, OE, SS and TF identification models are applied as single input single output (SISO) for each wheel individually. Each model will be evaluated to choose the best one that can provide an accurate model of the four wheels. The obtained validation results with the unseen data for each wheel are shown in Figs. 17–20.

Based on the obtained validation result, a comparison between each model is proposed in Tables 1–6.

Tables 1–6 concluded that the TF model is able to achieve the best validation result for the unseen data compared with other models. Consequently, it will be applied to the vehicle system as MISO. By observing the pole-zero configuration, the TF model can be tuned. The obtained results demonstrate that the model is able to achieve 88.44% of the output data as shown in Fig. 21, which is considered good enough to identify the vehicle model.

Consequently, the obtained model will be as follows:

$$G(s)_{Total} = G_{R1}(s)\,u_{R1} + G_{R2}(s)\,u_{R2} + G_{L1}(s)\,u_{L1} + G_{L2}(s)\,u_{L2}$$

where

$$G_{R1}(s) = \frac{-3.453\ s - 0.694\ 6}{s^2 + 0.176\ 2\ s + 0.132\ 3} \tag{8}$$

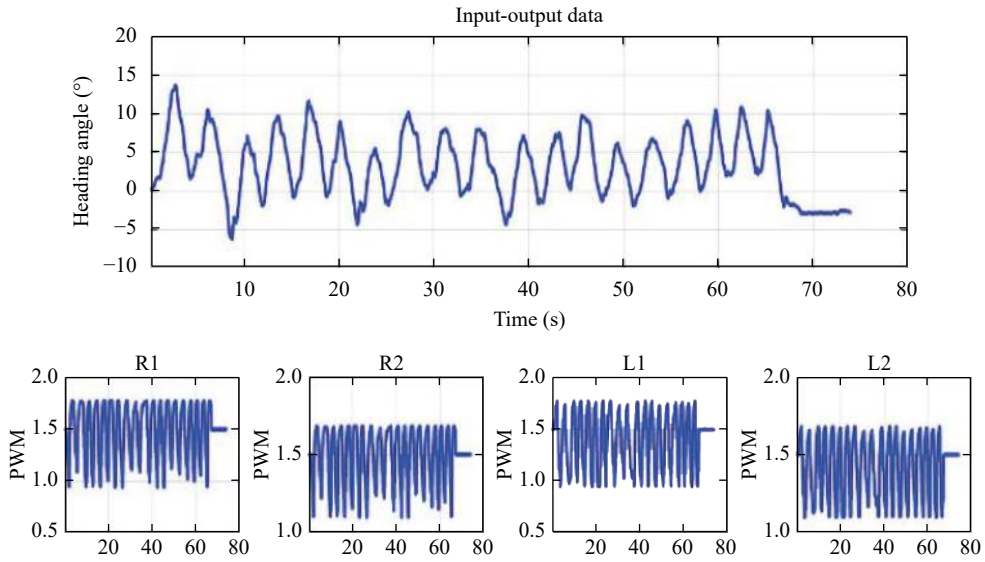

Fig. 15 Experiment results for the recorded input and output signals

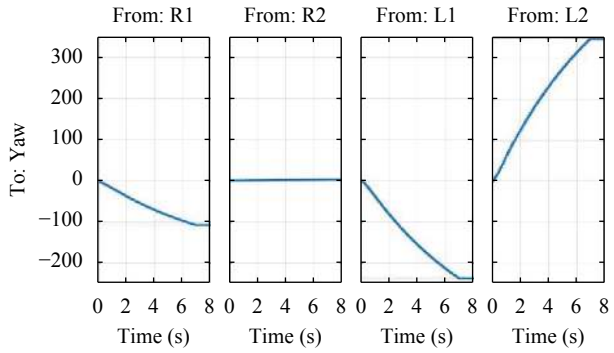

Fig. 16 Step responses for estimated dynamics for each channel

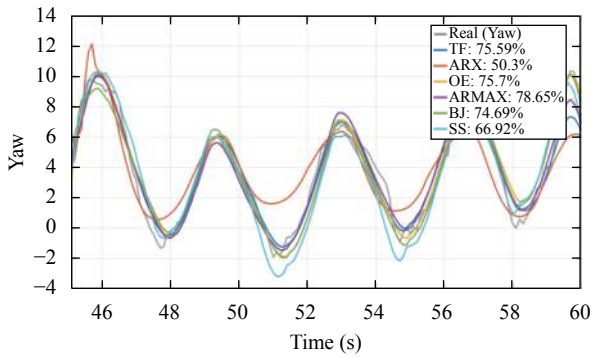

Fig. 17 Fit to estimation result for the SI models for the R1

$$G_{R2}(s) = \frac{-7.118\ s + 1.158}{s^2 + 0.388\ s + 0.309\ 9} \tag{9}$$

$$G_{L1}(s) = \frac{5.76\ s + 0.118\ 2}{s^2 + 0.271\ 4\ s + 0.108\ 3} \tag{10}$$

$$G_{L2}(s) = \frac{7.382\ s + 0.825\ 8}{s^2 + 0.548\ 1\ \mathrm{s} + 0.288\ 7}. \tag{11}$$

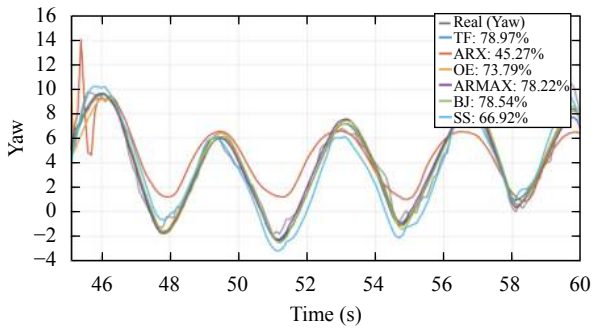

Fig. 18 Fit to estimation result for the SI models for the R2

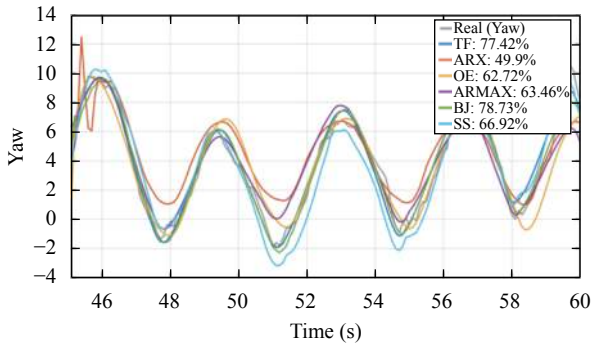

Fig. 19 Fit to estimation result for the SI models for the L1

5 Fuzzy logic controller design

In this section, the controller design is based on the Mamdani-fuzzy approach that allows the vehicle to follow the desired heading angle as discussed. FLC is considered a new addition to control theory. Its design philosophy deviates from all the previous methods by accommodating expert knowledge in controller design. The FLC has three functional processes as follows: 1) fuzzification,

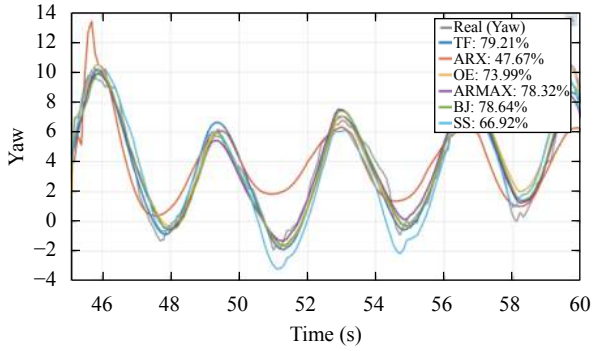

Fig. 20 Fit to estimation result for the SI models for the L2

Table 1 ARX model results

ARX model	Model parameterization	Validation data
R1	(5 5 4)	50.3%
R2	(5 5 4)	45.27%
L1	(5 5 4)	49.9%
L2	(5 5 4)	47.67%

Table 2 ARMAX model results

ARMAX model	Model parameterization	Validation data
R1	(3 3 3 2)	78.65%
R2	(3 3 3 2)	78.22%
L1	(3 3 3 2)	63.46%
L2	(3 3 3 2)	78.32%

Table 3 BJ model results

BJ model	Model parameterization	Validation data
R1	(3 3 3 2 2)	74.69%
R2	(3 3 3 3 2)	78.59%
L1	(3 3 3 3 2)	78.73%
L2	(3 3 3 3 2)	78.64%

Table 4 OE model results

OE model	Model parameterization	Validation data
R1	(3 3 2)	75.7%
R2	(3 3 2)	73.79%
L1	(3 3 2)	62.72%
L2	(3 3 2)	73.99%

Table 5 TF model results

TF model	Model parameterization	Validation data
R1	(4 3)	75.59%
R2	(4 3)	78.97%
L1	(4 3)	77.42%
L2	(4 3)	79.21%

Table 6 SS model results

SS model	Model parameterization	Validation data
R1, R2, L1, L2	(*A*,*B*,*C*,*D*)	66.92%

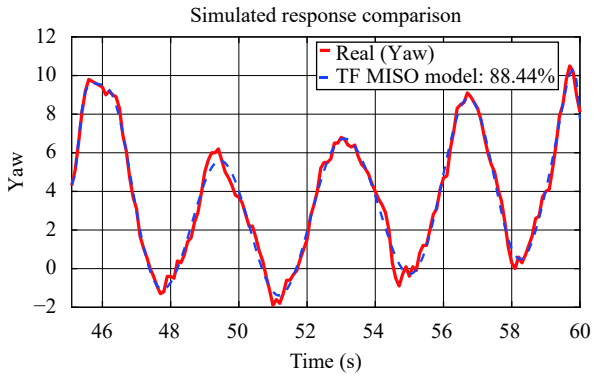

Fig. 21 Original heading angle and estimated response of the identified model

2) rule evaluator, 3) defuzzification. These three processes can be described as follows.

Fuzzification is the process of transforming the numerical variable into a linguistic variable (fuzzy number). This process can be achieved by using different types of fuzzifiers (membership functions), such as triangular, trapezoidal membership functions, etc. The rule evaluation process is the step in which, using fuzzification, the input process is mapped to conduct the fuzzy reasoning process. Defuzzification is the reverse process of fuzzification. The rules of the fuzzy controller generate appropriate outputs as linguistic variables, then it is converted into a crisp set in order to be applied to the real system.

Based on the obtained vehicle model transfer functions as discussed above, the fuzzy logic feedback control system is shown in Fig. 22. Designing a FLC requires obtaining the proper fuzzy rules and membership functions due to the vehicle behavior. Consequently, four FLCs are developed to control the steering of the front four wheels of the vehicle to follow the desired heading angle. The vehicle heading angle error is the controller input, while the PWM for the wheels is the controller output. The recorded input/output data shown in Fig. 14 have the benefit of defining the appropriate FLC rules.

Triangular and trapezoidal membership functions are used to define the input/output variables. The input/output variables for each controller are defined by five membership functions *NB*, *N*, *Z*, *P* and *PB* as shown in Fig. 23.

The obtained result of the closed loop system response is shown in Fig. 24. The steady state error reaches zero and the settling time is 0.03 s with the uncontrolled model. In addition, the peak time is 0.023 s, rise time is 0.017 s, and the steady state error is 0.004. In order to evaluate the developed controller for tracking the desired heading angle. First, a predefined heading angle man-

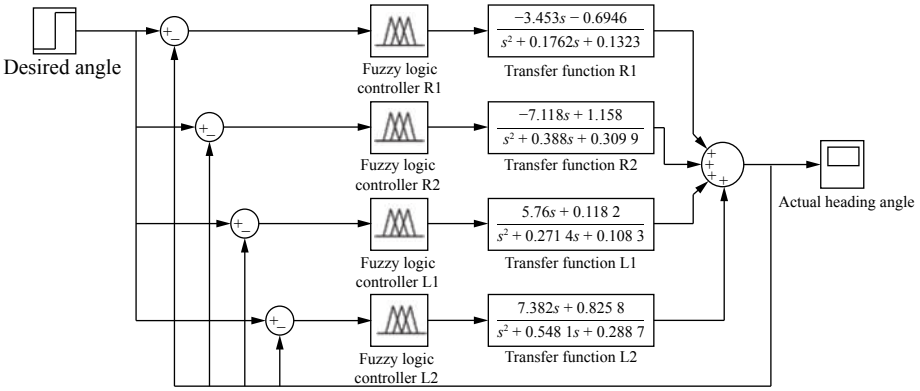

Fig. 22 Fuzzy heading angle controller Simulink diagram for the R1, R2, L1, L2

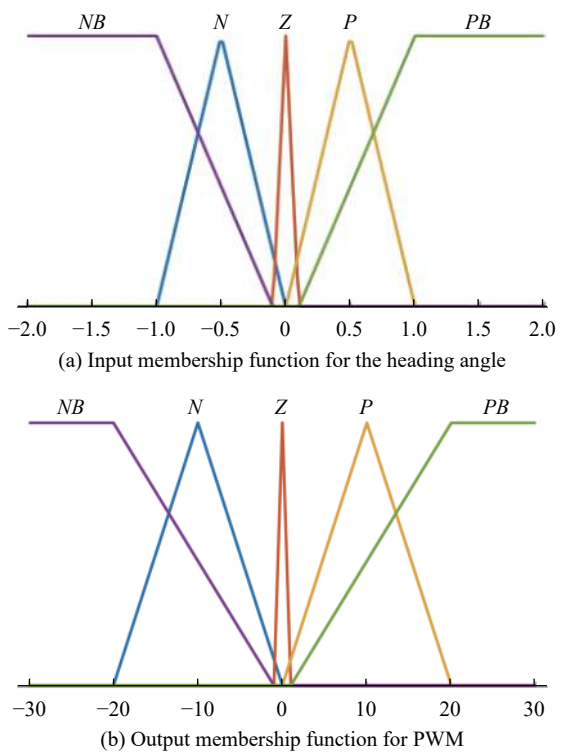

Fig. 23 Fuzzy controller

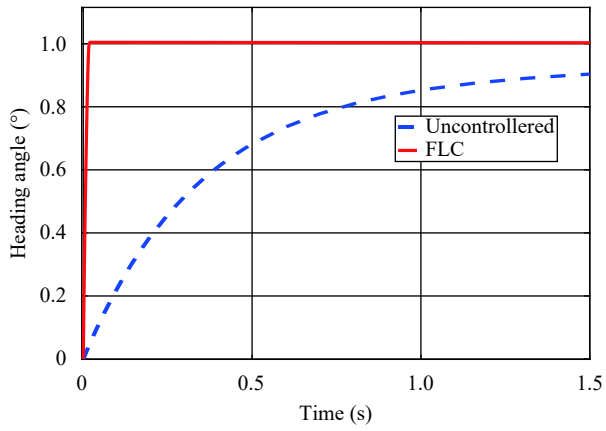

Fig. 24 Closed loop system step response

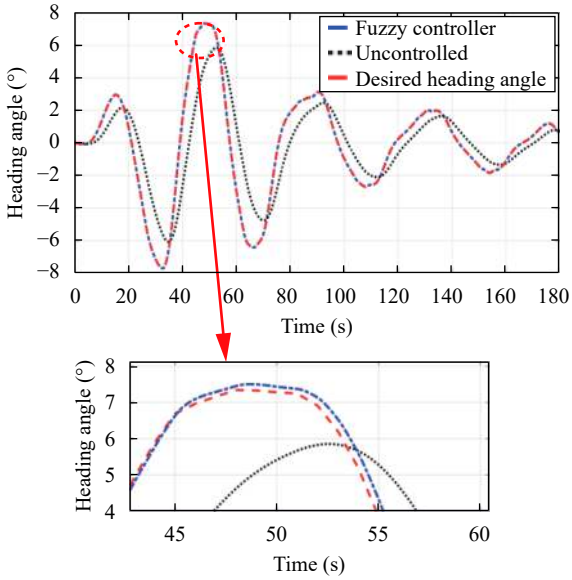

Fig. 25 Heading angle tracking using FLC

euver will be proposed as an input to the system. Subsequently, the developed FLCs based on the identified model will calculate the appropriate control signal to track the desired heading.

The obtained result shown in Fig. 25 clarifies that the proposed FLC has the capability to follow the desired heading angle with a very small error compared with the uncontrolled system.

6 Conclusions

This paper discussed the development and modeling of a remotely operated scaled multi-wheeled combat vehicle using system identification techniques. The vehicle was developed to simulate and analyze the characteristics of the full-size model. It is an electric-powered 1: 6 scale model of an 8×8 combat vehicle. It has eight wheels which are independently driven by electric motors. The vehicle has the capability to steer on multiple surfaces such as sand, dirt, snow, mud, and pavement.

An experimental test was carried out which was tested on an open loop system for measuring the input/output

signals. The input/output signals are recorded and analyzed. Several system identification models were applied in terms of ARMAX, ARX, OE, BJ, SS and TF models. The validation results revealed that the TF model provided an accurate ROMWCV model. The fit to estimation and validation process was verified using real data which achieved 88.44% of the output data. Based on the identified model, a FLC was applied to control the vehicle heading angle by controlling the steering of the front four wheels. The results of the simulations illustrate that the identified vehicle model and the developed FLC are indeed effective and feasible, which has the capability to follow the desired heading angle.

Acknowledgements

The authors wish to express their gratitude to the Egyptian Armed Forces for the financial support extended to the undergraduate and graduate students of the Vehicle Dynamics and Crash Research (VDCR) Laboratory for operating the vehicle during the experimental tests.

References

[1] A. Fisher. Google's Self-driving Cars: A Quest for Acceptance, [Online], Available: http://www.popsci.com/cars/article/2013-09/google-self-driving-car, 2014.

[2] A. M. Kessler. Elon Musk Says Self-Driving Tesla Cars Will Be in the U. S. by Summer, The New York Times, [Online], Available: https://www.nytimes.com/2015/03/20/business/elon-musk-says-self-driving-tesla-cars-will-be-in-the-us-by-summer.html?_r=0, 2015.

[3] K. J. Åström, P. Eykhoff. System identification – a survey. *Automatica*, vol. 7, no. 2, pp. 123–162, 1971. DOI: 10.1016/0005-1098(71)90059-8.

[4] Y. Liu, M. S. Hasan, H. N. Yu. Modelling and remote control of an excavator. *International Journal of Automation and Computing*, vol. 7, no. 3, pp. 349–358, 2010. DOI: 10.1007/s11633-010-0514-8.

[5] I. Rano, R. Iglesias. Application of systems identification to the implementation of motion camouflage in mobile robots. *Autonomous Robots*, vol. 40, no. 2, pp. 229–244, 2016. DOI: 10.1007/s10514-015-9449-9.

[6] I. A. Raptis, K. P. Valavanis, W. A. Moreno. System identification and discrete nonlinear control of miniature helicopters using backstepping. *Journal of intelligent and Robotic Systems*, vol. 55, no. 2–3, pp. 223–243, 2009. DOI: 10.1007/s10846-008-9295-5.

[7] C. West, A. Montazeri, S. D. Monk, D. Duda, C. J. Taylor. A new approach to improve the parameter estimation accuracy in robotic manipulators using a multi-objective output error identification technique. In *Proceedings of the 26th International Symposium on Robot and Human Interactive Communication*, Lisbon, Portugal, pp. 1406–1411, 2017. DOI: 10.1109/ROMAN.2017.8172488.

[8] M. Li, H. P. Wu, H. Handroos, Y. B. Wang, A. Loving, O. Crofts, M. Coleman, R. Skilton, G. Burroughes, J. Keep. RACE RM Control Team. Dynamic model identification method of manipulators for inside DEMO engineering. *Fusion Engineering and Design*, vol. 124, pp. 638–644, 2017. DOI: 10.1016/j.fusengdes.2017.02.034.

[9] K. Park, Y. Choi. System identification method for robotic manipulator based on dynamic momentum regressor. In *Proceedings of the 12th IEEE International Conference on Control and Automation*, Kathmandu, Nepal, pp. 755–760, 2016, DOI: 10.1109/ICCA.2016.7505369.

[10] A. T. Abdulsadda, K. Iqbal. An improved SPSA algorithm for system identification using fuzzy rules for training neural networks. *International Journal of Automation and Computing*, vol. 8, no. 3, pp. 333–339, 2011.

[11] R. Wilensky. *An Extensive Review on Generator Excitation System Modeling, Design, and Parameter Identification*, Finland: HAL CCSD, 2016.

[12] F. Ding. Combined state and least squares parameter estimation algorithms for dynamic systems. *Applied Mathematical Modelling*, vol. 38, no. 1, pp. 403–412, 2014. DOI: 10.1016/j.apm.2013.06.007.

[13] S. X. Jing, T. H. Pan, Z. M. Li. Recursive Bayesian algorithm for identification of systems with non-uniformly sampled input data. *International Journal of Automation and Computing*, vol. 15, no. 3, pp. 335–344, 2018. DOI: 10.1007/s11633-017-1073-z.

[14] S. H. Mousavian, H. R. Koofigar. Identification-based robust motion control of an AUV: Optimized by particle swarm optimization algorithm. *Journal of Intelligent & Robotic Systems*, vol. 85, no. 2, pp. 331–352, 2017. DOI: 10.1007/s10846-016-0401-9.

[15] X. J. Wu, X. L. Wu, X. Y. Luo. Adaptive neural network dynamic surface control for a class of nonlinear systems with uncertain time delays. *International Journal of Automation and Computing*, vol. 13, no. 4, pp. 409–416, 2016. DOI: 10.1007/s11633-015-0945-3.

[16] R. Ortega, M. W. Spong. Adaptive motion control of rigid robots: A tutorial. *Automatica*, vol. 25, no. 6, pp. 877–888, 1989. DOI: 10.1016/0005-1098(89)90054-X.

[17] M. Moradi, H. Malekizade. Neural network identification based multivariable feedback linearization robust control for a two-link manipulator. *Journal of Intelligent & Robotic Systems*, vol. 72, no. 2, pp. 167–178, 2013. DOI: 10.1007/s10846-013-9827-5.

[18] J. P. Noël, G. Kerschen. Nonlinear system identification in structural dynamics: 10 more years of progress. *Mechanical Systems and Signal Processing*, vol. 83, pp. 2–35, 2017. DOI: 10.1016/j.ymssp.2016.07.020.

[19] H. Richter, D. Simon, W. A. Smith, S. Samorezov. Dynamic modeling, parameter estimation and control of a leg prosthesis test robot. *Applied Mathematical Modelling*, vol. 39, no. 2, pp. 559–573, 2015. DOI: 10.1016/j.apm.2014.06.006.

[20] M. Gautier, W. Khalil. Exciting trajectories for the identification of base inertial parameters of robots. *The International Journal of Robotics Research*, vol. 11, no. 4, pp. 362–375, 1992. DOI: 10.1177/027836499201100408.

[21] M. Bisheban, T. Lee. Computational geometric system identification for the attitude dynamics on SO(3). In *Proceedings of American Control Conference*, Seattle, USA, pp. 2249–2254, 2017. DOI: 10.23919/ACC.2017.7963287.

[22] B. R. J. Haverkamp, C. T. Chou, M. H. Verhaegen, R. Jo-

hansson. Identification of continuous-time MIMO state space models from sampled data, in the presence of process and measurement noise. In *Proceedings of the 35th IEEE Conference on Decision and Control*, Kobe, Japan, pp. 1539–1544, 1996. DOI: 10.1109/CDC.1996.572741.

[23] Y. H. Eng, K. M. Teo, M. Chitre, K. M. Ng. Online system identification of an autonomous underwater vehicle via in-field experiments. *IEEE Journal of Oceanic Engineering*, vol. 41, no. 1, pp. 5–17, 2016. DOI: 10.1109/JOE.2015.2403576.

[24] A. Garg, K. Tai, B. N. Panda. System identification: Survey on modeling methods and models. In *Proceedings of International Conference on Artificial Intelligence and Evolutionary Computation in Engineering Systems*, Springer, Singapore, pp. 607–615, 2017. DOI: 10.1007/978-981-10-3174-8.

[25] Y. C. Lai, Q. L. Tri. System identification and control of a small unmanned helicopter at hover mode. In *Proceedings of the 2nd International Conference on Control and Robotics Engineering*, Bangkok, Thailand, pp. 92–96, 2017. DOI: 10.1109/ICCRE.2017.7935049.

[26] E. P. Mendes, A. A. D. Medeiros. Identification of quasi-linear dynamic model with dead zone for mobile robot with differential drive. In *Proceedings of Latin American Robotics Symposium and Intelligent Robotic Meeting*, Sao Bernardo do Campo, Brazil, pp. 132–137, 2010. DOI: 10.1109/LARS.2010.36.

[27] Z. Hasiewicz, P. L. Śliwiński, G. Mzyk. Nonlinear system identification under various prior knowledge. *IFAC Proceedings Volumes*, vol. 41, no. 2, pp. 7849–7858, 2008.

[28] S. Faddel, A. A. S. Mohamed, O. A. Mohammed. Fuzzy logic-based autonomous controller for electric vehicles charging under different conditions in residential distribution systems. *Electric Power Systems Research*, vol. 148, pp. 48–58, 2017. DOI: 10.1016/j.epsr.2017.03.009.

[29] Fahmizal, C. H. Kuo. Trajectory and heading tracking of a mecanum wheeled robot using fuzzy logic control. In *Proceedings of International Conference on Instrumentation, Control and Automation*, Bandung, Indonesia, pp. 54–59, 2016. DOI: 10.1109/ICA.2016.7811475.

[30] Z. Q. Cao, F. Shen, C. Zhou, N. Gu, S. Nahavandi, D. Xu. Heading control for a robotic dolphin based on a self-tuning fuzzy strategy. *International Journal of Advanced Robotic Systems*, vol. 13, no. 1, pp. 1–8, 2016. DOI: 10.5772/62289.

[31] A. M. Rao, K. Ramji, B. S. K. S. S. Rao, V. Vasu, C. Puneeth. Navigation of non-holonomic mobile robot using neuro-fuzzy logic with integrated safe boundary algorithm. *International Journal of Automation and Computing*, vol. 14, no. 3, pp. 285–294, 2017. DOI: 10.1007/s11633-016-1042-y.

[32] W. Pedrycz. *Fuzzy Sets Engineering*, Boca Raton, USA: CRC Press, 1995.

[33] Z. J. Wang, J. W. Zhang, Y. L. Huang, H. Zhang, A. S. Mehr. Application of fuzzy logic for autonomous bay parking of automobiles. *International Journal of Automation and Computing*, vol. 8, no. 4, pp. 445–451, 2011. DOI: 10.1007/s11633-011-0602-4.

[34] G. Antonelli, S. Chiaverini, G. Fusco. A fuzzy-logic-based approach for mobile robot path tracking. *IEEE Transactions on Fuzzy Systems*, vol. 15, no. 2, pp. 211–221, 2007. DOI: 10.1109/TFUZZ.2006.879998.

[35] S. Sahoo, S. C. Subramanian, N. Mahale, S. Srivastava. Design and development of a heading angle controller for an unmanned ground vehicle. *International Journal of Automotive Technology*, vol. 16, no. 1, pp. 27–37, 2015. DOI: 10.1007/s12239-015-0003-8.

[36] H. Tan, J. Iacobellis, A. Levenko, R. Mutiger, K. Ng, J. Averill. Design and Development of 8×8 Electric Combat Vehicle. Capstone Systems poroject final Engineering Report, Department of Mechanical Engineering, University of Ontario Institute of Technology, Canada, 2017.

[37] L. Lennart. *System Identification: Theory for the User*, 2nd ed., New Jersey, USA: Prentice Hall, 1999.

A. N. Ouda received the B. Sc., M. Sc. and Ph. D. degrees in electrical engineering from Military Technical College, Egypt in 1999, 2002 and 2012. He is currently an associate professor in Department of Guidance and Control, Electrical Engineering, the Military Technical College (MTC), Egypt. He has extensive contributions to the field of missile guidance and control.

His research interests include missile guidance and control, automatic control, and system identification.

E-mail: ahmed.ouda@uoit.ca

ORCID iD: 0000-0003-3398-1426

Amr Mohamed received the B. Sc. degree in electrical engineering from Military Technical College, Egypt in 2006, the M. Sc. degree in control systems from the Military Technical College, Egypt in 2012. He is a Ph. D. degree candidate in the electrical engineering program at the Faculty of Engineering and Applied Science, University of Ontario Institute of Technology, Canada. His master thesis versed on design robust controller for guided Missiles.

His research interests include path planning, obstacle avoidance, automatic flight control, autonomous navigation.

E-mail: amr.mohamed@uoit.net (Corresponding author)

ORCID iD: 0000-0002-2185-6153

Moustafa El-Gindy is a professor of automotive engineering in Department of Automotive, Mechanical and Manufacturing Engineering, Faculty of Engineering and Applied Science at University of Ontario Institute of Technology (UOIT), Canada. He has extensive contributions to the field of automotive engineering. He is the founder and editor-in-chief of *International Journal of Heavy Vehicle Systems*, a fellow of the American Society of Mechanical Engineers (ASME) and former Chair of the ASME Vehicle Design Committee.

His research interests include articulated heavy vehicles, bus testing and simulation, crash testing and simulations, high-velocity impact and ballistics simulation, multi wheels military vehicles dynamics, self-steering axles simulation, tire mechanics, tire-soft and hard soils interaction, vehicle dynamics and virtual human modelling.

E-mail: moustafa.el-gindy@uoit.ca

Haoxiang Lang received the B.Sc. degree from Ningbo University, China in 2003, the M.Sc. degree in mechanical engineering from the University of British Columbia, Canada in 2008, and the Ph.D. degree in mechanical engineering from University of British Columbia, Canada in 2012. He worked in the Motorola Cellular Equipment Company as a software engineering from January 2004 to September 2005. He was with the Industrial Automation Laboratory as a postdoctoral research fellow and the laboratory manager between November 2012 and December 2014. He is current an assistant professor of Mechanical Engineering Department and the director of the Intelligent Mechatronics and Robotics Laboratory at University of Ontario Institute of Technology (UOIT), Canada.

His research interests include mechatronics, robotics and machine learning.

E-mail: haoxiang.lang@uoit.ca

Jing Ren received the B.Sc. degree in electrical engineering from Shandong University, China in 1993, and the M.Sc. and Ph.D. degrees in electrical engineering from Western University, Canada in 2003 and 2005. She has published over 50 journal and conference papers and is the recipient of University Faculty Award in 2006.

Her research interest is mechanical engineering.

E-mail: jing.ren@uoit.ca